


# CRISPR/Cas9-Mediated Generation of *COL7A1*-Deficient Keratinocyte Model of Recessive Dystrophic Epidermolysis Bullosa

Farzad Alipour, Ph.D.<sup>1,2</sup>, Mana Ahmadraji, M.Sc.<sup>2</sup>, Elham Yektadoust, M.Sc.<sup>2</sup>, Parvaneh Mohammadi, Ph.D.<sup>2,3</sup>, Hossein Baharvand, Ph.D.<sup>2,4</sup>, Mohsen Basiri, Ph.D.<sup>2,5\*</sup> 

1. Department of Applied Cell Sciences, Faculty of Basic Sciences and Advanced Medical Technologies, Royan Institute, ACECR, Tehran, Iran
2. Department of Stem Cells and Developmental Biology, Cell Science Research Center, Royan Institute for Stem Cell Biology and Technology, ACECR, Tehran, Iran
3. Experimental Medicine and Therapy Research, University of Regensburg, Regensburg, Germany
4. Department of Developmental Biology, School of Basic Sciences and Advanced Technologies in Biology, University of Science and Culture, Tehran, Iran
5. Advanced Therapy Medicinal Product Technology Development Center (ATMP-TDC), Royan Institute for Stem Cell Biology and Technology, ACECR, Tehran, Iran

## Abstract

**Objective:** Recessive dystrophic epidermolysis bullosa (RDEB) is a genetic skin fragility and ultimately lethal blistering disease caused by mutations in the *COL7A1* gene which is responsible for coding type VII collagen. Investigating the pathological mechanisms and novel candidate therapies for RDEB could be fostered by new cellular models. The aim of this study was to employ CRISPR/Cas9 technology in the development of immortalized *COL7A1*-deficient keratinocyte cell lines intended for application as a cellular model for RDEB in *ex vivo* studies.

**Materials and Methods:** In this experimental study, we used transient transfection to express *COL7A1*-targeting guide RNA (gRNA) and Cas9 in HEK001 immortalized keratinocyte cell line followed by enrichment with fluorescent-activated cell sorting (FACS) via GFP expressing cells (GFP<sup>+</sup> HEK001). Homogenous single-cell clones were then isolated, genotyped, and evaluated for type VII collagen expression. We performed a scratch assay to confirm the functional effect of *COL7A1* knockout.

**Results:** We achieved 46.1% ( $P < 0.001$ ) efficiency of in/del induction in the enriched transfected cell population. Except for 4% of single nucleotide insertions, the remaining in/dels were deletions of different sizes. Out of nine single expanded clones, two homozygous and two heterozygous *COL7A1*-deficient cell lines were obtained with defined mutation sequences. No off-target effect was detected in the knockout cell lines. Immunostaining and western blot analysis showed lack of type VII collagen (*COL7A1*) protein expression in these cell lines. We also showed that *COL7A1*-deficient cells had higher motility compared to their wild-type counterparts.

**Conclusion:** We reported the first isogenic immortalized *COL7A1*-deficient keratinocyte lines that provide a useful cell culture model to investigate aspects of RDEB biology and potential therapeutic options.

**Keywords:** *COL7A1*, CRISPR/Cas9, Keratinocyte, Recessive Dystrophic Epidermolysis Bullosa

**Citation:** Alipour F, Ahmadraji M, Yektadoust E, Mohammadi P, Baharvand H, Basiri M. CRISPR/Cas9-mediated generation of *COL7A1*-deficient keratinocyte model of recessive dystrophic epidermolysis bullosa. *Cell J.* 2023; 25(10): 665-674. doi: 10.22074/CELLJ.2023.1989321.1225

This open-access article has been published under the terms of the Creative Commons Attribution Non-Commercial 3.0 (CC BY-NC 3.0).

## Introduction

Epidermolysis bullosa (EB) is a group of inherited skin blistering diseases, characterized by fragility of the skin due to defective epithelial cell adhesion leading to blister, erosion, and ulcers (1). In this group of diseases, 16 genes have thus far been detected that their protein expressions in keratinocyte and fibroblast participated in the cell cytoskeleton and extracellular matrix. According to phenotypic heterogeneity, there are four main subtypes including EB simplex (EBS), junctional EB (JEB), dystrophic EB (DEB), and Kindler syndrome (2). The

severest form of these diseases is recessive dystrophic EB (RDEB), caused by loss of function mutations in *COL7A1*, the gene coding for type VII collagen protein (3). This protein is the main component of anchoring fibrils which is crucial for the adherence of the dermal-epidermal basement membrane. Mutations in *COL7A1* cause a variety of severities where truncated forms manifest a relatively milder forms and complete lack of the protein results in severest forms of RDEB (4).

Experimental studies on rare genetic disorders, such as

Received: 07/February/2023, Revised: 15/June/2023, Accepted: 06/August/2023

\*Corresponding Address: P.O.Box: 16635-148, Department of Stem Cells and Developmental Biology, Cell Science Research Center, Royan Institute for Stem Cell Biology and Technology, ACECR, Tehran, Iran

Email: [basiri@royaninstitute.org](mailto:basiri@royaninstitute.org)



Royan Institute  
Cell Journal (Yakhteh)

RDEB confront ethical and practical challenges including paucity of available stable patient donors, technical inconsistency in sampling and cell isolation, patient discomfort, and variability in the severity of disease between patients (5). Moreover, obtaining RDEB primary cells are mostly challenging due to inefficient and labor-consuming isolation, expansion, and limited proliferation capacity. These show the need for cell lines which could easily be handled for experimental purposes (6). Although animal models are available for EB disorders, they exhibit some shortcomings such as imperfection in development, stillbirth, and deficiency in the recapitulation of disease phenotype (7). Therefore, there is a need to establish new cellular RDEB models to study pathological pathways and evaluate potential therapeutic approaches.

Gene editing technologies, such as clustered regularly interspaced short palindromic repeats (CRISPR)/CRISPR associated protein 9 (Cas9) technology, have provided a straightforward means to introduce mutations to normal cells for modeling purposes. Site-specific double-strand break (DSB) induced by CRISPR/Cas9 complex undergoes the error-prone non-homologous end joining (NHEJ) DNA repair, which may result in insertion-deletion (in/del) mutations. A portion of in/del mutations causes frameshift or other types of detrimental changes in the gene sequence (8). Introducing mutations to the disease-related genes in the context of a normal cell line has been used as a powerful method to generate isogenic cellular models for different diseases (9-14).

The aim of this study was to generate immortalized COL7A1-deficient keratinocytes, as a cellular model for RDEB, using CRISPR/Cas9 technology. Since truncated COL7A1 mutants represent mild manifestations of the disease and might hamper future investigations on exogenous type VII collagen therapeutics, we aimed to eliminate expression of the whole protein by targeting the first exon. The resultant COL7A1-deficient keratinocyte cell lines were then characterized in terms of genotype and type VII collagen expression.

## Materials and Methods

### Guide RNA design and construction

To induce frameshift on the transcription sequence of COL7A1, we designed one guide RNA (gRNA; 5'-ACTGCCTAGGATGACGCTG-3') targeting the first exon of COL7A1 gene, based on minimal off-target activity by CRISPOR online bioinformatic tool (15). Designed complementary sense (ghCOL7A1-S) and antisense (ghCOL7A1-A) oligonucleotides (Table S1, See Supplementary Online Information at [www.celljournal.org](http://www.celljournal.org)) incubated to hybridize together and constitute a double-strand oligonucleotide. The hybridized double-stranded (ghCOL7A1-S+ghCOL7A1-A) DNA fragment cloned into the Esp3I (BsmBI) restriction sites of the LentiCRISPRv2GFP (Addgene plasmid # 82416) using a simultaneous digestion-ligation reaction as described previously (16). Briefly, a mixture of 10 pmol of the insert

DNA fragment, 1 µg of LentiCRISPRv2GFP plasmid, 5 units of Esp3I enzyme, 1 unit of T4 DNA ligase, 1 µl of 10X FastDigest buffer, and 1 µl of 10X T4 DNA ligase buffer (all reagents from Thermo Fisher Scientific, USA) in a total volume of 20 µl was incubated in 37°C for 3 hours. The reaction product containing the recombinant plasmid (LentiCRISPRv2GFP-ghCOL7A1) was transformed into chemo-competent *E. coli* cells. Restriction mapping and sequencing were done on single clones for verification of the correct gRNA sequence in the vector.

### Cell culture

Immortalized keratinocyte (HEK001) cell line (CRL-2404, ATCC) was cultured on DMEM/F12 medium (Thermo Fisher Scientific), containing 10% (v/v) fetal bovine serum (Thermo Fisher Scientific), 2 mM GlutaMAX (Thermo Fisher Scientific), 1% (v/v) NEAA (Thermo Fisher Scientific), 1% (v/v) Pen/Strep (Thermo Fisher Scientific) and supplemented with KGM-GoldsingleQuots (Lonza, Switzerland), containing Bovine pituitary extract (BPE), insulin (5 mg/ml), epidermal growth factor (EGF, 10 ng/ml), epinephrine, hydrocortisone (0.4 mg/ml), transferrin (17). The cells were incubated at 37°C in a 5% (vol/vol) CO<sub>2</sub> incubator during the performance of experiments.

### Transfection of HEK001 cells

HEK001 cells were cultured in a 100 mm culture dish to reach 70-90% confluency. Two to three hours before transfection, the media was replaced with a fresh complete medium without antibiotics. HEK001 cells were transfected with LentiCRISPRv2GFP-ghCOL7A1 plasmid using lipofectamine 2000 Transfection Reagent (Thermo Fisher Scientific) according to the manufacturer's instructions. Briefly, a transfection medium was prepared by adding 24 µg of vector and 24 µl of lipofectamine 2000 to 1 ml base medium of DMEM/F12 in two separate tubes followed by 10 minutes incubation. The vector-containing medium was added to the lipofectamine tube and incubated for another 15 minutes. Transfection medium was added to cells gently and incubated overnight. The next day, the medium was replaced with a fresh keratinocyte growth medium and the cells were grown for another 36 hours. All incubation was done at 37°C in a humidified 5% (vol/vol) CO<sub>2</sub> incubator.

### Single-cell clone isolation

Since in our hand, single HEK001 cells had reduced viability right after FACS isolation, we used a limited dilution method (18, 19) to obtain single-cell clones. Two days after transfection by LentiCRISPRv2GFP-ghCOL7A1 plasmid, around 2×10<sup>5</sup> HEK001 cells expressed GFP (GFP<sup>+</sup> HEK001) isolated by FACS Aria II cell sorter (BD Biosciences, USA) and cultured in one well of a 24-well plate. When 70-90% confluency was reached, the cells were detached by trypsin (Thermo Fisher Scientific), counted, and serially diluted in complete media to obtain a cell suspension of 5 cells/

ml. Then, 100  $\mu$ l of this suspension was manually seeded in each well of a 96-well plate to obtain an average of 0.5 cells per well. The wells containing truly single cells were determined using an inverted microscope (Olympus, Japan). Selected single-cell clones were then serially expanded into 48-, 24-, 12-, and 6-well plates for downstream analyses.

### Sanger sequencing and targeting efficiency assessment

Genome extraction was done with a commercial genome extraction kit (Favorgen Biotech Corporation, Taiwan) according to the manufacturer's instructions. Briefly, 106 cells were resuspended in the lysis buffer of the kit and incubated for 10 minutes to obtain clear cell lysate. Genomic DNA was isolated from the cell lysate using silica columns and washing buffers provided in the kit. The gRNA target region was amplified by polymerase chain reaction (PCR) using COL7A1-F1 and COL7A1-R1 primers (Table S1, See Supplementary Online Information at [www.celljournal.org](http://www.celljournal.org)) with the following PCR condition: 95°C for 10 minutes, 35 cycles of 95°C for 30 seconds, 60°C for 30 seconds, 72°C for 45 seconds and then 72°C for 10 minutes. The PCR product was subjected to Sanger sequencing using COL7A1-F2 and COL7A1-R2 primers (Table S1, See Supplementary Online Information at [www.celljournal.org](http://www.celljournal.org)). Sequencing data were analyzed for insertion/deletion events and targeting efficiency using the Tracking of in/dels by Decomposition (TIDE) analysis method (20).

### Off-target prediction and sequencing

Potential off-target sites in the human genome were predicted using CRISPOR bioinformatic tool (15). Four off-target sites in the exonic regions of *FAT3*, *ANKZF1*, *AXIN2*, and *NPHP4* genes were evaluated with PCR and sequencing. PCR program was done as follows: 95°C for 10 minutes, 35 cycles of 95°C for 30 seconds, 60°C for 30 seconds, and 72°C for 45 seconds, followed by a final extension step at 72°C for 10 minutes. The PCR products were subjected to Sanger sequencing. The primers used for the PCR and sequencing reactions are listed in Table S1 (See Supplementary Online Information at [www.celljournal.org](http://www.celljournal.org)).

### Immunofluorescence staining

The cells were fixed with paraformaldehyde 4% at 4°C for 20 minutes, washed three times with phosphate buffer saline (PBS) containing 0.05% Tween 20 (PBST, Sigma, Germany), and then permeabilized with 0.5% Triton X-100 (Sigma) at room temperature for 10 minutes. Blocking was performed with goat serum 10% at 37°C for 60 minutes and incubated with rabbit polyclonal antibody against type VII collagen (ab93350, Abcam, UK) at 1:100 dilution, for overnight at 4°C. The following day, the cells were incubated with Alexa Fluor 546-conjugated goat anti-rabbit secondary antibody (A11035, Thermo Fisher Scientific) at 1:500 dilution for 45 minutes at room temperature, and subsequently, nuclei were stained with

DAPI 20 mg/ml (Sigma). The cells were analyzed by Olympus IX71S1F-3 inverted fluorescence microscope (Olympus, Japan) equipped with a 100 W Mercury light source (Olympus) as a source of excitation radiation and Olympus U-TV0.63XC image acquisition system. The staining observed by 10X objective lenses for GFP (excitation 460-490 nm, emission 520 nm, exposure time 500 mseconds), Alexa Fluor 546 (excitation 510-555 nm, Emission 590 nm, exposure time 500 mseconds) in exposure time (500 mseconds) and DAPI (excitation 330-385 nm, emission 420 nm, exposure time 10 mseconds).

### Western blot analysis

To extract total protein, cell pellets were lysed by adding cell lysis buffer (7 M urea, 2 M thiourea, 4% CHAPS, 30 mM Tris, 40 mM dithiothreitol) and 1X cocktail protease inhibitor, vortexing for 5 minutes on ice, sonicating for 5 minutes on ice, followed by centrifuging at 14000 g for 15 minutes and transferring the supernatant to new tubes. Protein concentration was measured by pierce BCA assay (Thermo Fisher Scientific). Protein samples were denatured at 50°C for 60 minutes in 50  $\mu$ l 5X loading buffer [Laemmle 5X buffer: 0.5 M Tris-HCl, pH=6.8, 10% glycerol, 2% sodium dodecyl sulfate (SDS), 0.025% bromophenol blue and 50 mM dithiothreitol], then separated by loading on 8% SDS-polyacrylamide gel electrophoresis (SDS-PAGE), 100 V, 2 hours, followed by electrotransfer to polyvinylidene fluoride membranes at 15 V and 15°C, overnight. Membranes were blocked with 2% BSA in Tris-buffered saline containing 0.05% Tween (TBST) 20 at room temperature for 2 hours, followed by adding primary antibody rabbit anti-COL7A1 (ab93350, Abcam) at 1:1000 dilution in TBST and they were subsequently incubated overnight. A polyclonal  $\beta$ -tubulin antibody (sc15335, Santa Cruz, USA) at 1:1000 dilution served as loading control. The next day, after washing three times in TBST 0.1%, the blots were incubated at room temperature for 1 hour, with HRP-conjugated donkey anti-rabbit secondary antibody at 1:50000 dilution in TBST, followed by three washes. To detect the desired band, SuperSignal West Femto Maximum Sensitivity substrate (Thermo Scientific) was added, and Chemiluminescent signals were captured by the Alliance Q9 Advanced Uvitec System (UVitec Ltd, UK).

### Statistical analysis

TIDE analysis uses a built-in two-tailed t test of the variance-covariance matrix of the standard errors to calculate p-values for the frequency of each in/del mutation (20). To compare the normalized percentage of cell-free area in the scratch assay, we performed a two-way ANOVA followed by Sidak's multiple comparison test using GraphPad Prism 8.0.2 (GraphPad Software Inc., USA). The adjusted P values less than 0.01 were considered statistically significant.

### Ethics approval

The study was approved by the Ethical Committee

of Royan Institute (Tehran, Iran) -Academic Center for Education, Culture, and Research (IR.ACECR.ROYAN.REC.1398.076).

## Results

### Guide RNA Design and generation of COL7A1 knockout HEK001 cells

To knock out the *COL7A1* gene in HEK001 immortalized keratinocytes, we designed a gRNA targeting the first exon of the gene. The corresponding sequence subcloned under a U6 promoter in an expression plasmid vector containing Cas9 coding sequence linked to GFP through a self-splitting 2A linker (Fig.1A, B). Transfection of HEK001 cells by this vector resulted in a population of GFP<sup>+</sup> cells with a transduction efficiency of 14.1 % (Fig.1C). To enrich the gene-modified cells GFP<sup>+</sup> cells were isolated by FACS (Fig.1D).

### Sequencing analysis of the pool population of transfected cells

To assess targeting efficiency in the transfected HEK001 cells, genomic DNA of the isolated GFP<sup>+</sup> cells was extracted and PCR amplicon spanning gRNA targeted site was sequenced by Sanger sequencing. Results showed a composite sequence trace after the break site resulted from the presence of in/del mutations in the pool population of the transfected cells (Fig.2A). Decomposition of the sequence trace data (Fig.2B) showed that overall editing (in/del) efficiency was 46.1% (P<0.001) with more frequent deletion events compared to nucleotide insertions (Fig.2C). We did not detect insertion of more than one nucleotide in the bulk population. Single nucleotide insertion was observed in 4.0% (P<0.001) of the sequences, containing either T or A nucleotide insertions (Fig.2D).

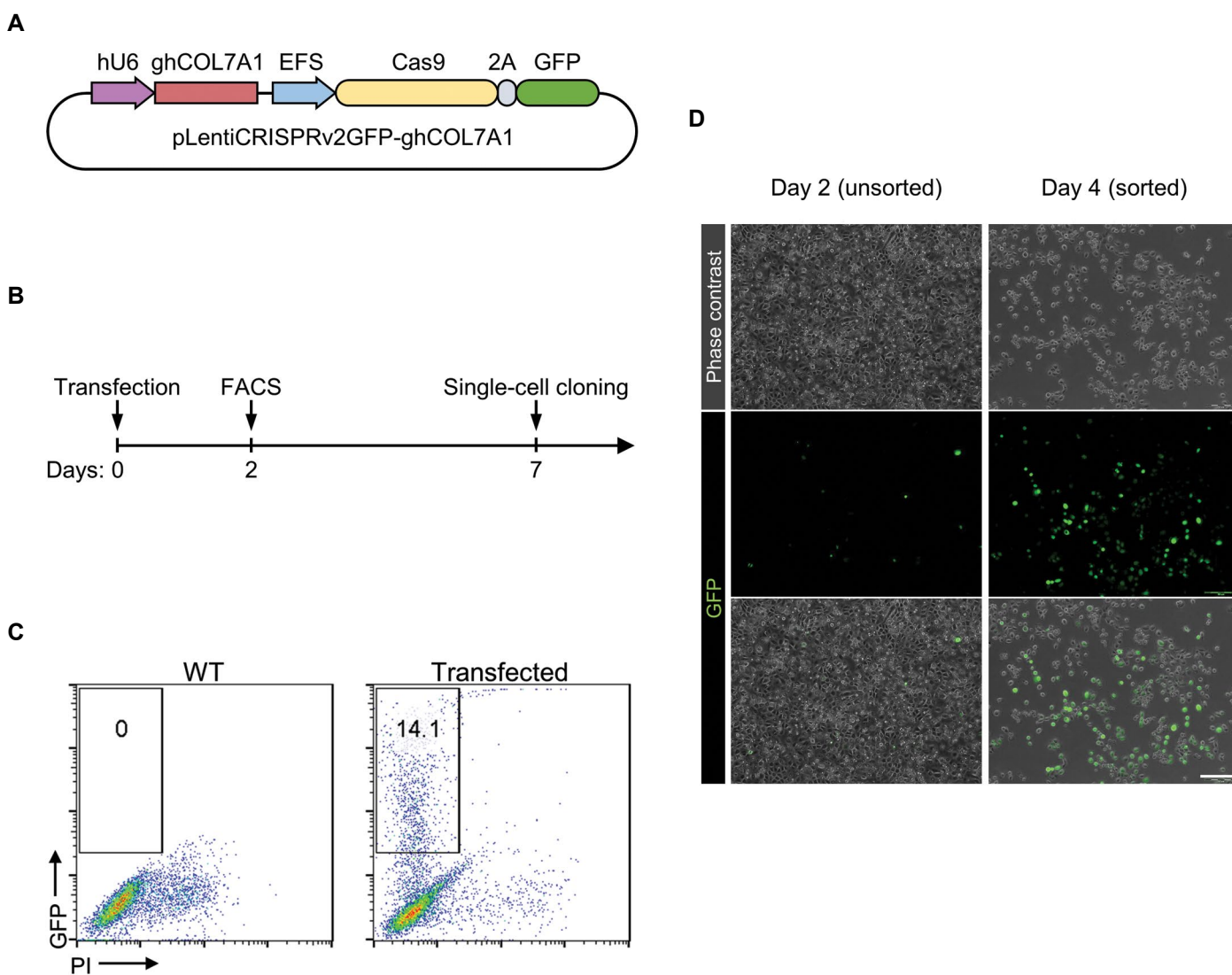


**Fig.1:** Transfection and isolation of GFP<sup>+</sup> cells. **A.** Schematic map of the CRISPR plasmid vector. gRNA was inserted in expression vector encompassing Cas9 and GFP sequence under U6 promoter. **B.** Diagram of the experimental procedure showing transfection, enrichment by fluorescence-activated cell sorting (FACS), and single-cell cloning by limited dilution. **C.** Viable GFP-expressing cells comprising 14% of the transfected keratinocytes were sorted to enrich the genome-edited cell population. **D.** Fluorescent microscopy of the pool population of cells, two days after transfection (before sorting), and enriched GFP<sup>+</sup> cells, two days after sorting (scale bar: 50 μm).

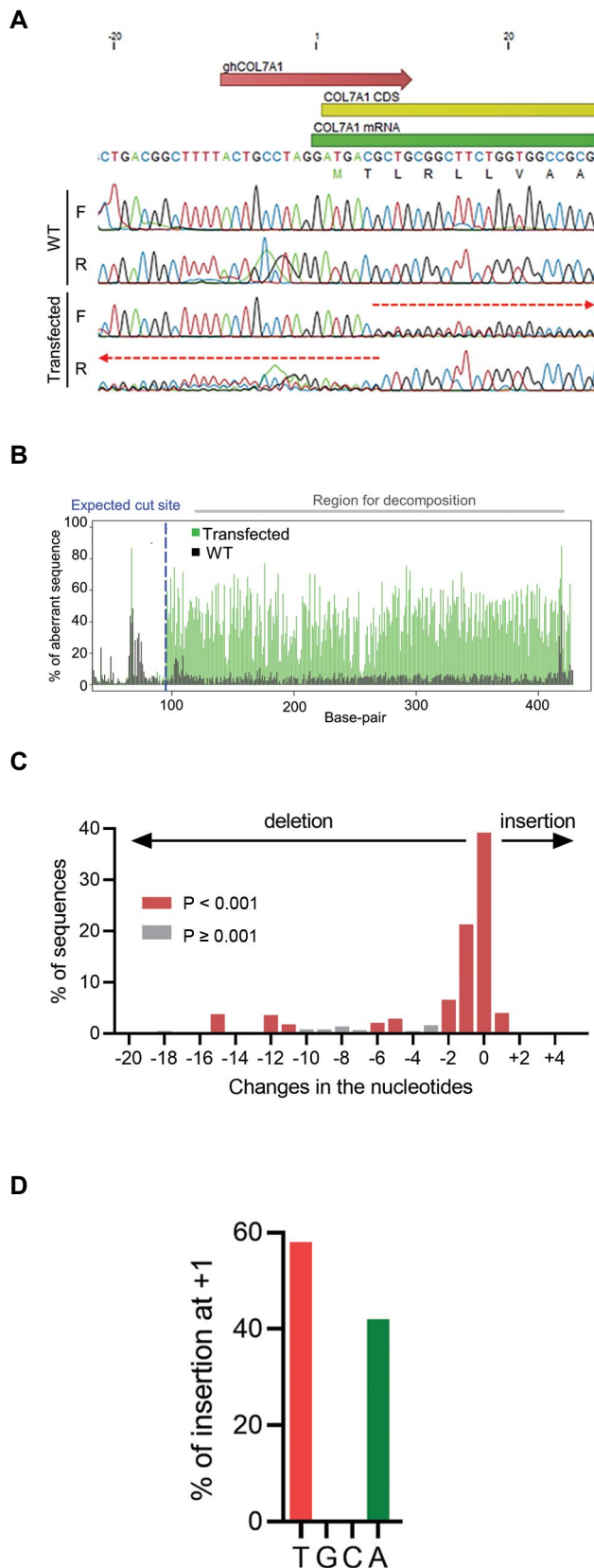


**Fig.2:** Sanger sequencing and decomposition analysis on the bulk population of transfected HEK001 cells. **A.** Sequencing on the bulk population of the transfected cells represents a composite sequence trace after the break site based on the direction of the indicated primer. **B.** Comparison of transfected bulk with untransfected cells revealed aberrant sequence after the break site. **C.** Decomposition analysis of changes in the targeted region shows frequency of mutations based on the number of nucleotides deleted from or inserted into the sequence. **D.** Out of all single nucleotide insertions, 58% was T and 42% was A. F; Forward primer, R; Reverse primer, and WT; Wild-type.

## Sequencing analysis of the single-cell clones

To establish a homogeneous cell line with identified sequence, we isolated single-cell clones from the bulk transfected sequence. Out of 25 clones initially obtained from two 96-well plates, only nine showed normal expansion and they were subjected to further molecular analyses. Decomposition analysis of the target genomic sequence in these nine clones (Fig.3A) showed that only one clone (B6) contained the intact wild-type allele, while in three clones (B2, O3, and T7) more than two alleles were detected. Clone B1 showed a heterozygous genotype with single nucleotide insertion in one allele and an in-frame 15-nucleotide deletion in the other. The above-mentioned clones were excluded from the study, due to the presence of wild-type sequences, in-frame mutations, or possible heterogeneity. However, four other clones (namely clones B4, T5, T6, and T8) showed genotypes compatible with the complete abolition of the *COL7A1* function. Clones B4 and T8 had heterozygous genotypes with deleterious frameshift mutations in the both alleles (Fig.3B, C). A single-nucleotide deletion at positions +9 (ninth nucleotide after the transcription start site) and a two-nucleotide deletion at positions +7 to +8 in clone B4 and a single-nucleotide deletion at position +7 in clone T8 introduced frameshifts into the *COL7A1* coding sequence which resulted in altered amino acid sequence and ectopic stop codons. The second allele of clone T8 had a 7-nucleotide deletion (positions +1 to +7) eliminating the start codon. Clones T5 and T6 showed homozygous deletion of, respectively, 33 nucleotides (positions -26 to +8) and 32 nucleotides (positions -21 to +12) encompassing both the transcription start site and start codon of *COL7A1* gene (Fig.3C).

## Off-target analysis

To ensure that the selected clones do not contain undesirable mutations due to the off-target activity of the CRISPR system, we performed an in-silico off-target prediction. Among 70 predicted off-target sites with four or fewer mismatched nucleotides (Table S2, See Supplementary Online Information at [www.celljournal.org](http://www.celljournal.org)), only four were located in exonic sequences of *FAT3*, *ANKZF1*, *AXIN2*, and *NPHP4* genes, hence carrying the risk of unwanted mutations in a coding sequence. However, PCR-sequencing of these potential exonic off-target sites in the *COL7A1*-knockout cell lines showed no mutation when compared to the wild-type sequence (Fig.4).

## Type VII collagen protein expression in selected knockout clones

Immunofluorescent staining was used to confirm the *COL7A1*-KO cell lines at the protein level. No expression of type VII collagen (*COL7A1*) was observed in the four clones selected in genotyping compared to the wild-type HEK001 keratinocytes in immunostaining and Western blot analysis results (Fig.5A, B). These results verified *COL7A1* deficiency predicted at sequence level on the four selected cell lines.



### Evaluation of cellular motility in the knockout cell lines

Since loss of *COL7A1* deficiency is associated with increased cellular motility, and elevated risk of keratinocyte malignancy as well as invasiveness in RDEB patients (21-23), we sought to measure cell motility in our

*COL7A1*-KO HEK001 model, as a functional indicator of *COL7A1* gene disruption. Using a scratch assay, we observed that the *COL7A1*-knockout HEK001 cells exerted significantly higher migration compared to the wild-type cells (Fig.6A, B).

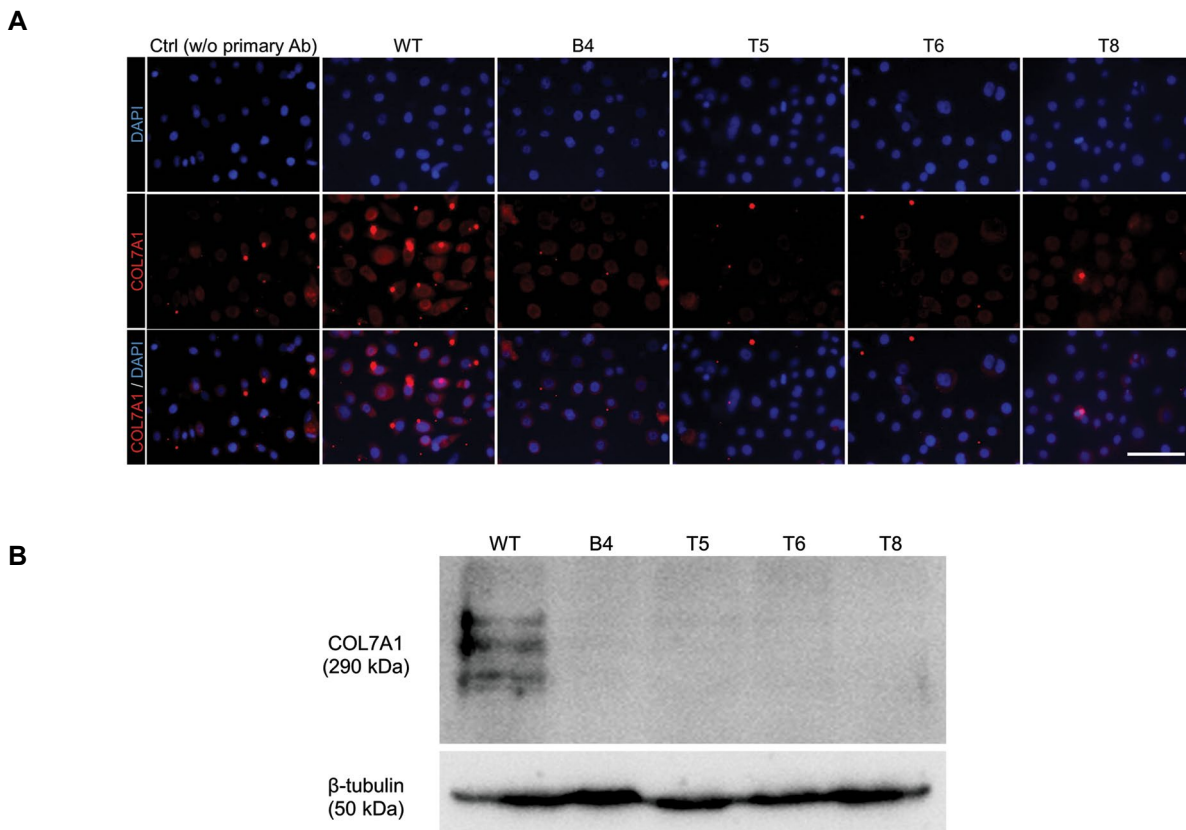


**Fig.5:** Evaluation of *COL7A1* protein expression in the *COL7A1*-knockout HEK001 cell lines. **A.** Four knockout cell lines (B4, T5, T6, and T8) were stained with type VII collagen (*COL7A1*)-specific antibody along with wild-type (WT) HEK001 cells. *COL7A1* protein expression was not detected in any of the knockout cell lines as compared to the WT cells. A representative negative control without primary antibody (Ctrl w/o primary Ab) was included for comparison (scale bar: 100  $\mu$ m). **B.** Western blot analysis of *COL7A1* protein expression in the wild-type and knockout HEK001 cell lines. Human  $\beta$ -tubulin served as an internal control.

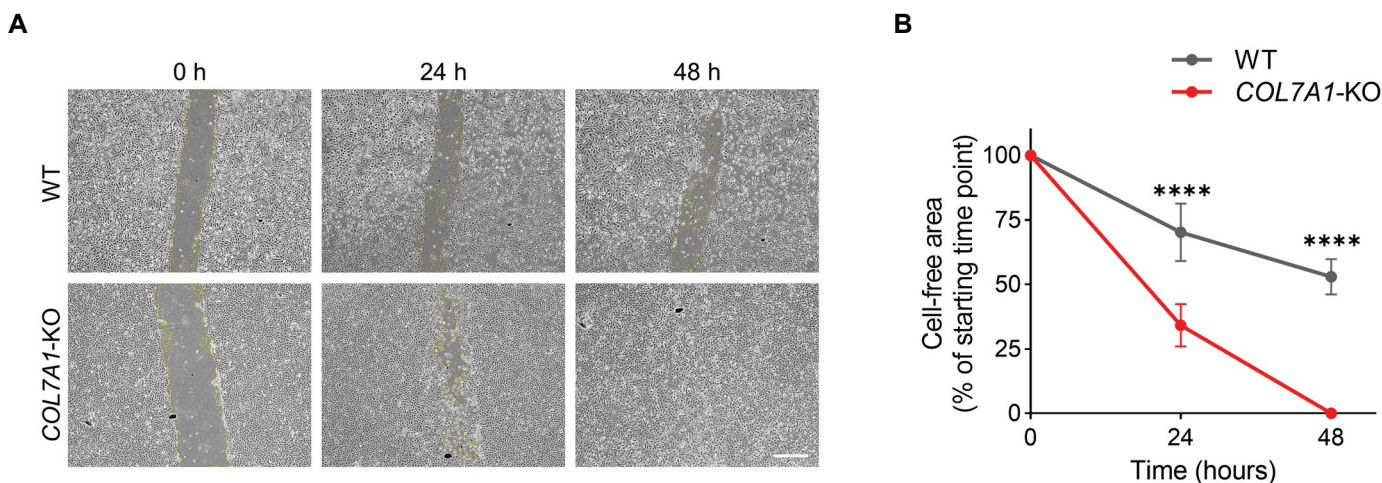


**Fig.6:** Assessment of cell motility by scratch assay in the wild-type (WT) and *COL7A1*-KO cells. **A.** Representative microscopic images of WT and one of the *COL7A1*-KO HEK001 cell lines (T6) at 0, 24, and 48 hours after wounding (scale bar: 100  $\mu$ m). **B.** Quantitative comparison of cell migration and wound closure in WT and *COL7A1*-KO groups showed that *COL7A1*-KO HEK001 cells had obtained higher cell motility. Data presented as a percentage of the cell-free area of the starting time point  $\pm$  SD (n=3). \*\*\*\*;  $P < 0.0001$  and h; Hour.

## Discussion

Investigation of rare diseases, like EB, has challenges with the availability of the proper patients and ethical issues as well as practical difficulties, such as sampling, primary cell culture, and division potency of disease-specific cells. To obviate these problems, genetic modification in the desired gene to generate the disease model is favorable. In this study, we generated four immortalized keratinocyte cell lines harboring different characterized mutations of the *COL7A1* gene which can be used as a cellular model of RDEB.

The human *COL7A1* gene spans through more than 31 kb of chromosome 3 with 118 exons encoding a long polypeptide (around 2,944 amino acids) that gives rise to type VII collagen (24). Hundreds of *COL7A1* mutations have been detected in RDEB patients resulting in a variety of clinical manifestations with most severe forms correlating with the complete absence of the whole protein (25). Although amino acid substitution and truncated mutants can be found in some patients, these forms of the protein might be detected by antibody-based assays and therefore interferes with experimental investigations. Hence, to generate a straightforward experimental tool, we chose to completely eliminate type VII collagen expression by targeting the first exon in the proximity of the start codon and the transcription start site. The results showed that this strategy successfully resulted in the generation of multiple mutations in four generated cell lines, however, we showed that all four selected cell lines lacked the expression of *COL7A1* protein. In the functional level, increased motility of the *COL7A1*-knockout cells was in line with the previous findings showing that RDEB keratinocytes had higher motility associated with increased susceptibility to keratinocyte malignancies in RDEB patients (21-23).

*COL7A1* gene is expressed in both dermal fibroblasts and keratinocytes, while the latter is responsible for the majority of type VII collagen expressed in the skin (26). Therefore, several investigational cellular and molecular therapeutic strategies targeted keratinocytes in RDEB. Patient-derived immortalized keratinocytes have been generated as a cellular model for EB simplex (27) and RDEB (6). Although valuable for several studies, these cell lines lack the isogenic healthy counterparts. One disadvantage of patient-derived cell models compared to our approach is that they lack an isogenic control. Immortalized keratinocyte cell lines, derived from healthy donors, especially the HEK001 cell line, have been extensively characterized and used as valuable models for studying keratinocytes (28, 29). On the other hand, gene editing technologies, such as CRISPR/Cas9, can be readily applied to generate targeted mutations in human cells. This approach has been also used in skin-related studies to investigate several biological functions, such as keratinocyte development and homeostasis (30), signal transduction (31), adhesion (32), and epithelial differentiation (33, 34). In line with this approach, we employed CRISPR/Cas9 technology to generate new

*COL7A1*-deficient HEK001 immortalized keratinocytes which closely resemble RDEB keratinocytes.

Although mouse models of RDEB have been generated and used for in vivo studies, rodent keratinocytes do not fully resemble human counterparts in terms of molecular mechanisms involved in EB, such as apoptotic and inflammatory pathways (35, 36). Targeting *COL7A1* by CRISPR/Cas9 in human primary keratinocytes has also been reported as a method to generate RDEB cellular model (7, 37). Whilst this method has the advantage of using primary keratinocytes, it has also some potential limitations, including the limited lifespan of primary keratinocytes, relatively labor-intensive procedure, generation of heterogenous mutations, persistent expression of gRNA and Cas9 by the integrative lentiviral vector, and the possibility of off-target mutations. Additionally, the efficiency of *COL7A1* knockout using CRISPR/Cas9 nucleoprotein in primary human keratinocytes was reported around 40% (8), while our approach allowed for the generation of homogenous *COL7A1* knockout cell lines. On the other hand, the major limitation of our approach is that immortalized keratinocytes do not fully represent some keratinocyte characteristics (e.g. differentiation and proliferation) which should be considered for future application of this cellular model. Moreover, immortalized keratinocytes might not be suitable for some in vivo experiments due to their constant proliferation. However, despite its inherent limitations, our strategy provided a more accessible, robust, and homogenous cellular model that may address some of the shortcomings in other cellular and animal models.

## Conclusion

In this study, CRISPR/Cas9 technology was used to generate a keratinocyte model cell line for RDEB. The generated model cell lines not only can be used in experimental studies such as investigational cell and gene therapies, but also can potentially be applied to high-throughput screening of candidate drugs for symptomatic treatments such as wound healing, reduction in blister numbers, as well as amelioration of itch and pain. Moreover, our experimental strategy for CRISPR/Cas9-mediated gene editing in keratinocyte cell lines can be extended to the genes involved in the other types of EB, as well as the characterization and targeted modulation of pathogenic molecular cascades.

## Acknowledgments

This work was supported by the funds from Royan Institute. The authors indicated no potential conflicts of interest.

## Authors' Contributions

F.A., M.B.; Contributed to the design, implementation of the research, data analysis, and writing the manuscript. F.A., M.A., E.Y.; Carried out the experiments, contributed



to data analysis and interpretation. H.B., P.M.; Contributed to conceptualization of the study, interpreting the results, providing critical feedback, and finalizing the manuscript. All authors read and approved the final manuscript.

## References

- Has C, Nyström A, Saeidian AH, Bruckner-Tuderman L, Uitto J. Epidermolysis bullosa: Molecular pathology of connective tissue components in the cutaneous basement membrane zone. *Matrix Biol.* 2018; 71-72: 313-329.
- Reichelt J, Koller U, De Rosa L, De Luca M, Bauer JW. Advances on potential therapeutic options for epidermolysis bullosa. *Expert Opinion on Orphan Drugs.* 2018; 6(4): 283-293.
- Knaup J, Verwanger T, Gruber C, Ziegler V, Bauer JW, Krammer B. Epidermolysis bullosa - a group of skin diseases with different causes but commonalities in gene expression. *Exp Dermatol.* 2012; 21(7): 526-530.
- Titeux M, Izmiryan A, Hovnanian A. The molecular revolution in cutaneous biology: emerging landscape in genomic dermatology: new mechanistic ideas, gene editing, and therapeutic breakthroughs. *J Invest Dermatol.* 2017; 137(5): e123-e129.
- Afshar L, Aghayan HR, Sadighi J, Arjmand B, Hashemi SM, Basiri M, et al. Ethics of research on stem cells and regenerative medicine: ethical guidelines in the Islamic Republic of Iran. *Stem Cell Res Ther.* 2020; 11(1): 396.
- Chamorro C, Almaraz D, Duarte B, Llamas SG, Murillas R, García M, et al. Keratinocyte cell lines derived from severe generalized recessive epidermolysis bullosa patients carrying a highly recurrent COL7A1 homozygous mutation: models to assess cell and gene therapies in vitro and in vivo. *Exp Dermatol.* 2013; 22(9): 601-603.
- Fenini G, Grossi S, Contassot E, Biedermann T, Reichmann E, French LE, et al. Genome editing of human primary keratinocytes by CRISPR/Cas9 reveals an essential role of the NLRP1 inflammasome in UVB sensing. *J Invest Dermatol.* 2018; 138(12): 2644-2652.
- Kocher T, March OP, Bischof J, Liemberger B, Hainzl S, Klausegger A, et al. Predictable CRISPR/Cas9-mediated COL7A1 reframing for dystrophic epidermolysis bullosa. *J Invest Dermatol.* 2020; 140(10): 1985-1993. e5.
- Dabrowska M, Ciolak A, Kozłowska E, Fiszer A, Olejniczak M. Generation of new isogenic models of huntington's disease using CRISPR-Cas9 technology. *Int J Mol Sci.* 2020; 21(5): 1854.
- Kaneski CR, Hanover JA, Schueler Hoffman UH. Generation of an in vitro model for peripheral neuropathy in Fabry disease using CRISPR-Cas9 in the nociceptive dorsal root ganglion cell line 50B11. *Mol Genet Metab Rep.* 2022; 31: 100871.
- Martens MC, Edelkamp J, Seebode C, Schäfer M, Stähle S, Krohn S, et al. Generation and characterization of a CRISPR/Cas9-mediated SNAP29 knockout in human fibroblasts. *Int J Mol Sci.* 2021; 22(10): 5293.
- Muñoz SS, Garner B, Ooi L. Generation of APOE knock-down SK-N-SH human neuroblastoma cells using CRISPR/Cas9: a novel cellular model relevant to Alzheimer's disease research. *Biosci Rep.* 2021; 41(2): BSR20204243.
- Pavan E, Ormazabal M, Peruzzo P, Vaena E, Rozenfeld P, Dardis A. CRISPR/Cas9 editing for gaucher disease modelling. *Int J Mol Sci.* 2020; 21(9): 3268.
- Serrano LJ, Garcia-Arranz M, De Pablo-Moreno JA, Segovia JC, Olivera-Salazar R, Garcia-Olmo D, et al. Development and characterization of a factor V-deficient CRISPR cell model for the correction of mutations. *Int J Mol Sci.* 2022; 23(10): 5802.
- Concordet JP, Haeussler M. CRISPOR: intuitive guide selection for CRISPR/Cas9 genome editing experiments and screens. *Nucleic Acids Res.* 2018; 46(W1): W242-W245.
- Basiri M, Behmanesh M, Tahamtani Y, Khalooghi K, Moradmam A, Baharvand H. The convenience of single homology arm donor DNA and CRISPR/Cas9-nickase for targeted insertion of long DNA fragment. *Cell J.* 2017; 18(4): 532-539.
- Mohammadi P, Nilforoushzadeh MA, Youssef KK, Sharifi-Zarchi A, Moradi S, Khosravani P, et al. Defining microRNA signatures of hair follicular stem and progenitor cells in healthy and androgenic alopecia patients. *J Dermatol Sci.* 2021; 101(1): 49-57.
- Greenfield EA. Single-cell cloning of hybridoma cells by limiting dilution. *Cold Spring Harb Protoc.* 2019; 2019(11).
- Longo PA, Kavran JM, Kim MS, Leahy DJ. Single cell cloning of a stable mammalian cell line. *Methods Enzymol.* 2014; 536: 165-172.
- Brinkman EK, Chen T, Amendola M, van Steensel B. Easy quantitative assessment of genome editing by sequence trace decomposition. *Nucleic Acids Res.* 2014; 42(22): e168.
- Chen M, Kasahara N, Keene DR, Chan L, Hoeffler WK, Finlay D, et al. Restoration of type VII collagen expression and function in dystrophic epidermolysis bullosa. *Nat Genet.* 2002; 32(4): 670-675.
- Gache Y, Baldeschi C, Del Rio M, Gagnoux-Palacios L, Larcher F, Lacour JP, et al. Construction of skin equivalents for gene therapy of recessive dystrophic epidermolysis bullosa. *Hum Gene Ther.* 2004; 15(10): 921-933.
- Murauer EM, Gache Y, Gratz IK, Klausegger A, Muss W, Gruber C, et al. Functional correction of type VII collagen expression in dystrophic epidermolysis bullosa. *J Invest Dermatol.* 2011; 131(1): 74-83.
- Van Agtmael T, Bruckner-Tuderman L. Basement membranes and human disease. *Cell Tissue Res.* 2010; 339(1): 167-188.
- Kern JS, Kohlhase J, Bruckner-Tuderman L, Has C. Expanding the COL7A1 mutation database: novel and recurrent mutations and unusual genotype-phenotype constellations in 41 patients with dystrophic epidermolysis bullosa. *J Invest Dermatol.* 2006; 126(5): 1006-1012.
- Ryynänen J, Sollberg S, Parente MG, Chung LC, Christiano AM, Uitto J. Type VII collagen gene expression by cultured human cells and in fetal skin. Abundant mRNA and protein levels in epidermal keratinocytes. *J Clin Invest.* 1992; 89(1): 163-168.
- Morley SM, D'Alessandro M, Sexton C, Rugg EL, Navsaria H, Shemanko CS, et al. Generation and characterization of epidermolysis bullosa simplex cell lines: scratch assays show faster migration with disruptive keratin mutations. *Br J Dermatol.* 2003; 149(1): 46-58.
- Sugerman PB, Bigby M. Preliminary functional analysis of human epidermal T cells. *Arch Dermatol Res.* 2000; 292(1): 9-15.
- Bogen KT, Arnold LL, Chowdhury A, Pennington KL, Cohen SM. Low-dose dose-response for reduced cell viability after exposure of human keratinocyte (HEK001) cells to arsenite. *Toxicol Rep.* 2016; 4: 32-38.
- Dahlhoff M, Gaborit N, Bultmann S, Leonhardt H, Yarden Y, Schneider MR. CRISPR-assisted receptor deletion reveals distinct roles for ERBB2 and ERBB3 in skin keratinocytes. *FEBS J.* 2017; 284(19): 3339-3349.
- Gao S, Wang Z, Wang W, Hu X, Chen P, Li J, et al. The lysine methyltransferase SMYD2 methylates the kinase domain of type II receptor BMPR2 and stimulates bone morphogenetic protein signaling. *J Biol Chem.* 2017; 292(30): 12702-12712.
- Wanuske MT, Brantschen D, Schinner C, Stüde C, Walter E, Hirmaier M, et al. Clustering of desmosomal cadherins by desmoplakin is essential for cell-cell adhesion. *Acta Physiol (Oxf).* 2021; 231(4): e13609.
- James CD, Das D, Morgan EL, Otoa R, Macdonald A, Morgan IM. Werner syndrome protein (WRN) regulates cell proliferation and the human papillomavirus 16 life cycle during epithelial differentiation. *mSphere.* 2020; 5(5): e00858-e00820.
- Sobiak B, Leśniak W. Effect of SUV39H1 histone methyltransferase knockout on expression of differentiation-associated genes in HaCaT keratinocytes. *Cells.* 2020; 9(12): 2628.
- Sollberger G, Strittmatter GE, Grossi S, Garstkiewicz M, Auf dem Keller U, French LE, et al. Caspase-1 activity is required for UVB-induced apoptosis of human keratinocytes. *J Invest Dermatol.* 2015; 135(5): 1395-1404.
- Sand J, Haertel E, Biedermann T, Contassot E, Reichmann E, French LE, et al. Expression of inflammasome proteins and inflammasome activation occurs in human, but not in murine keratinocytes. *Cell Death Dis.* 2018; 9(2): 24.
- Grossi S, Fenini G, Hennig P, Di Filippo M, Beer HD. Generation of knockout human primary keratinocytes by CRISPR/Cas9. *Methods Mol Biol.* 2020; 2109: 125-145.